Passive Seismic Characterization of High Priority Salt Jugs near the V&S Railroad Right-of-Way in Hutchinson, Kansas

Shelby Peterie, Amanda Livers, Sarah Morton, Brandon Graham,
Brett Bennett, Brett Wedel, Bryan Brooks, Joey Fontana,
Yao Wang, Yuri Rupert, Julian Ivanov, and Richard Miller

Kansas Geological Survey
1930 Constant Avenue
Lawrence, KS 66047

Preliminary Report to

Ed Lindgren
Burns & McDonnell Engineering Company Inc.
9400 Ward Parkway
Kansas City, MO 64114
(816) 822-3595

Open-file Report 2015-31 August 2015

Passive Seismic Characterization of High Priority Salt Jugs near the V&S Railroad Right-of-Way in Hutchinson, Kansas

Executive Summary

This applied research project correlated measured shear-wave velocities with the condition of rock above dissolution voids, targeting the stress as related to shear wave velocity of the overburden. Shear-wave velocities were estimated using passive surface wave data acquired along a total of six profiles that intersected 26 abandoned brine production wells and in proximity to an additional five wells. Multi-channel analysis of surface waves (MASW) was used to estimate the shear-wave velocity, loosely map stratigraphic contacts above the top of the "three finger" dolomite, and evaluate the relative strength of the rock above possible salt jugs associated with the wells. Recommendations for further investigation are suggested where voids are suspected to have the potential for vertical migration.

Passive MASW profiles were acquired during four nights of data collection near the V&S railroad right-of-way in Hutchinson, Kansas, on March 16-19, 2015**.** Six lines and a 2-D grid of receivers were positioned over key wells. Continuous sampling was utilized to record and allow for evaluation of all available sources of passive source energy, ensuring optimal source orientation and surface wave characteristics for each line. Surface waves with frequencies as low as 3.5 Hz were recorded, with an average depth of investigation 55 meters (m), and in some locations exceeding 70 m, successfully sampling deep within bedrock.

With shear-wave velocity being a function of shear modulus and density, and the shear modulus as the ratio of stress over strain, it is possible to quantify relative stress of overburden rocks (shear modulus) by shear velocity values. Local increases in shear velocity without changes in lithology can be equated to increased stress associated with overburden roof load over dissolution jugs. Relative shear velocity lows may be associated with collapse features whose vertical movement has been arrested by bulking, reduced stress to within roof rock strength, or changes in strength due to geologic features related to natural variation in deposition or erosion.

Shear velocities in the majority of the study area represent a normal stress regime and natural geologic variation. Increased depths of investigation and maximum surface wave wavelengths were observed near wells 14B and 41, and between wells 17 and 42. Velocities are consistent with the shear-wave velocity trends expected for bedrock at this site and likely represent natural variability. However, these anomalous depths indicate that there is something unique to these areas, which may suggest elevated velocity at depth or an off-line anomaly. Future monitoring of these areas would enhance the dataset and increase confidence in the interpretation. Elevated shear-wave velocity above wells 8B, 15B, 46, and possibly well 92 suggests elevated stress and voids with under-supported roofs. The relative velocity and limited span of elevated stress implied by size of the anomalies suggest that the threat of failure is likely not imminent. We recommend these wells be included in future investigations at this site to monitor for possible changes in Vs associated with void dynamics.

Introduction

Material properties (specifically strength and stress accumulations) measured as a function of depth above abandoned salt jugs in Hutchinson, Kansas, appear related to the mobility and upward migration potential of these jugs. Localized escalation in stress (as indicated by increased shear-wave velocity) above subterranean voids is one indicator of an increased potential for roof failure and void migration (Eberhart-Phillips et al., 1989; Dvorkin et al., 1996; Khaksar et al., 1999; Sayers, 2004). Previous studies, using both active and passive seismic wavefield characteristics, suggest perturbations in the shear-wave velocity field immediately above voids can be correlated to characteristics of the unsupported roof spans of salt jugs in the Hutchinson area (Sloan et al., 2010).

The strength of individual rock layers can be qualitatively described in terms of stiffness/rigidity and empirically estimated from relative comparisons of shear-wave velocity measurements. Shear-wave velocity is directly proportional to stress and inversely related to non-elastic strain. Since the shear-wave velocity of earth materials changes when stress and any associated elastic strain on those materials becomes "large," it is reasonable to suggest load-bearing roof rock above mines or dissolution voids may experience elevated shear-wave velocities due to loading between pillars or, in the case of voids, loading between supporting side walls. This localized increase in shear velocity is not related to increased strength, but increased load as defined by Young's Modulus. High-velocity shear-wave "halos" encompassing low-velocity anomalies are suggested to be key indicators of near-term roof failure. All these phenomena have been observed within the overburden above voids in the Hutchinson Salt Member in Hutchinson, at depths greater than 30 m below the bedrock surface.

Previous research projects at the Carey Boulevard Research Area (CBRA) correlated measured shear-wave velocities with the condition of dissolution voids and the physical properties of the overburden at selected locations on Vigindustries legacy solution mining property in Hutchinson. Shear-wave velocities were estimated from passive surface-wave data acquired along eight profiles that intersected 13 wells. Two of these 13 wells had been the target of a previous seismic investigation completed in 2008. As a result of that 2008 study it was determined that the integrity of the overlying strata could be reasonably estimated using shear-wave seismic imaging. The 2008 study quantified the effectiveness of shear-wave velocity to estimate local stress above voids of the size and depth prevalent at the Vigindustries site in Hutchinson.

The lack of necessary ultra low-frequency surface waves in the recorded wavefield have negated attempts to use active source multi-channel analysis of surface waves (MASW) to estimate shear velocity in the lithified rocks near the top of bedrock (Miller et al., 2009). Uncontrolled, local industrial and transportation activities represent sound sources that have produced the necessary low frequencies and, when recorded and processed using passive methods, have extended the imaging depth to over 60 m (Miller, 2011). Key to this method is the ability to estimate shear-wave velocities to depths more than double those possible with standard active sources at a particular site (Park et al., 2004). Results of passive MASW studies near this site and other sites in Hutchinson suggest that this method is effective in identifying jugs with heightened risk for upward migration (Miller, 2011; Ivanov et al., 2013).

In this study, baseline profiles targeting wells and potential voids were acquired in March of 2015 within or immediately adjacent to the V&S railroad right-of-way. A total of six lines were acquired directly over 26 wells and in proximity to an additional five wells. Passive MASW processing resulted in six two-dimensional (2-D) shear-wave velocity (Vs) profiles indicative of the stress regime at the time of the survey. Possible areas of anomalous stress in

roofs are identified, and suspect jugs can be included in future monitoring programs to monitor void dynamics and determine if the voids in proximity to the V&S railroad are remaining static or experiencing change that might need further evaluation.

Geologic and Geophysical Setting

The Permian Hutchinson Salt Member occurs in central Kansas, northwestern Oklahoma, and the northeastern portion of the Texas Panhandle, and is prone to and has an extensive history of dissolution and formation of sinkholes (Figure 1). In Kansas, the Hutchinson Salt Member possesses an average net thickness of 75 m and reaches a maximum of over 150 m in the southern part of the basin. Deposition occurring during fluctuating sea levels caused numerous halite beds, 0.2 to 3 m thick, to be formed interbedded with shale, minor anhydrite, and dolomite/magnesite. Individual salt beds may be continuous for only a few miles despite the remarkable lateral continuity of the salt as a whole (Walters, 1978).

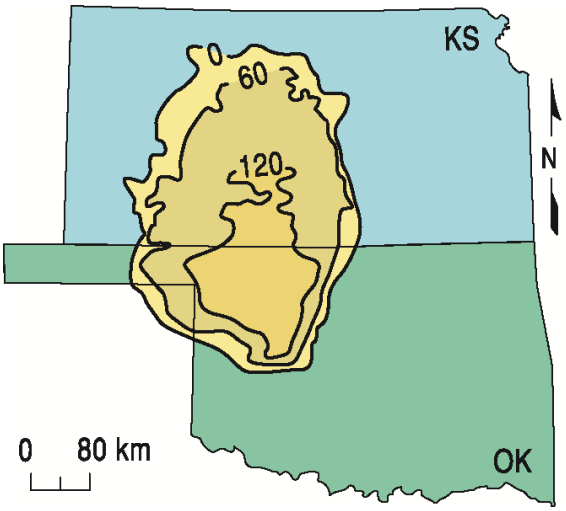

Figure 1. Approximate extent of salt formation, with contour intervals expressed in meters.

The distribution and stratigraphy of the salt is well documented (Dellwig, 1963; Holdoway, 1978; Kulstad, 1959; Merriam, 1963). The salt reaches a maximum thickness in central Oklahoma and thins to depositional edges on the north and west, erosional subcrop on the east, and facies changes on the south. The increasing thickness toward the center of the salt bed is due to a combination of increased salt, and more and thicker interbedded anhydrites. The Stone Corral Formation (a well-documented seismic marker bed) overlies the salt throughout Kansas (McGuire and Miller, 1989). Directly above the salt at this site is a thick sequence of Permian shale.

The upper 760 m of rock at this site is Permian shale (Merriam, 1963). The Chase Group (top at 300 m deep), lower Wellington Shale (top at 245 m deep), Hutchinson Salt (top at 120 m deep), upper Wellington Shale (top at 75 m deep), and Ninnescah Shale (top at 25 m deep) make up the packets of reflecting events easily identifiable and segregated within the Permian portion of the section (Figure 2). Bedrock is defined as the top of the Ninnescah Shale with the unconsolidated Pliocene-Pleistocene Equus beds making up the majority of the upper 30 m of sediment. The thickness of Quaternary alluvium that fills the stream valleys and paleosubsidence features goes from 0 to as much as 90 m, depending on the dimensions of the features.

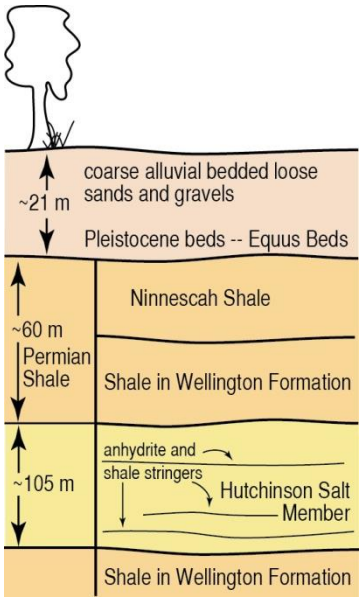

Figure 2. Generalized geology.

Recent dissolution of the salt and resulting subsidence of overlying sediments forming sinkholes has generally been associated with mining or saltwater disposal (Walters, 1978).

Historically, these sinkholes can manifest themselves as a risk to surface infrastructure. The rate of surface subsidence can range from gradual to very rapid. Besides risks to surface structures, subsidence features potentially jeopardize the natural segregation of ground-water aquifers, greatly increasing their potential to negatively impact the environment (Whittemore, 1989, 1990). Natural sinkholes resulting from dissolution of the salt by localized leaching within natural flow systems which have been altered by structural features (such as faults and fractures) are not uncommon west of the main dissolution edge (Merriam and Mann, 1957).

Caprock and its characteristics are a very important component of any discussion concerning dissolution, subsidence, and formation of sinkholes. The Permian shales (Wellington and Ninnescah) that overlay the Hutchinson Salt Member are about 60 m thick in this area and are characterized as generally unstable when exposed to freshwater, being susceptible to slough-ing and collapse (Swineford, 1955). These Permian shales tend to be red or reddish-brown and are commonly referred to as "red beds." Permian red beds are extremely impermeable to water and have provided an excellent seal between the freshwaters of the Equus beds and the extremely water-soluble Hutchinson Salt Member. The modern-day expanse and mere presence of the Hutchinson Salt is due to the protection from freshwater provided by these red beds.

Isolating the basal contact of the Wellington Formation provides key insights into the general strength of roof rock expected if dissolution-mined salt jugs (salt jugs are the jug-shaped cavities or voids in the salt that form after salt has been dissolution mined in proximity to the wells) reach the top of the salt zone. Directly above the salt/shale contact is an approximately 6 m-thick dark-colored shale with joint and bedding cracks filled with red halite (Walters, 1978). Once unsaturated brine comes in contact with this shale layer, these red halite-filled joints and bedding planes are rapidly leached, leaving an extremely structurally weak layer.

Field Layout and Data Acquisition

To ensure the highest quality data, receivers were deployed during the day and train data were recorded at night when cultural and industrial noise was minimal to provide optimum signal-to-noise. Analysis of the previous seismic energy sources captured during passive recording at this site clearly indicated trains from a distance of 3 kilometers (km) or more away provided the best broad spectrum, low-frequency seismic energy (Miller, 2011). Because seismic energy with characteristics best suited for the purpose of this study may arrive when trains are at a distance greater than they can be detected by spotters, seismic records were recorded continuously during acquisition to ensure that optimum data was recorded.

Data were acquired over four nights from March 15-19, 2015. Six seismic lines were deployed directly over or in proximity to a total of 31 wells, as well as a grid to determine the direction of passive seismic energy (Figure 3). Seismic receivers were single GeoSpace GS11D 4.5 Hz geophones spaced at 3 m intervals. The seismic lines varied in length (Table 1) totaling over 3.5 km. The 2-D monitoring grid consisted of 144 receivers spaced at 5 m intervals and was configured to form four concentric expanding squares with 10, 30, 50, and 70 m sides. Data were recorded during one night with a 500+ channel 24-bit Geometrics Geode distributed seismic system. Seismic records were 30 seconds (s) long with a 2 millisecond (ms) sampling interval. In total, 3483 seismic records equivalent to 90.7 gigabytes (Gb) of data were recorded.

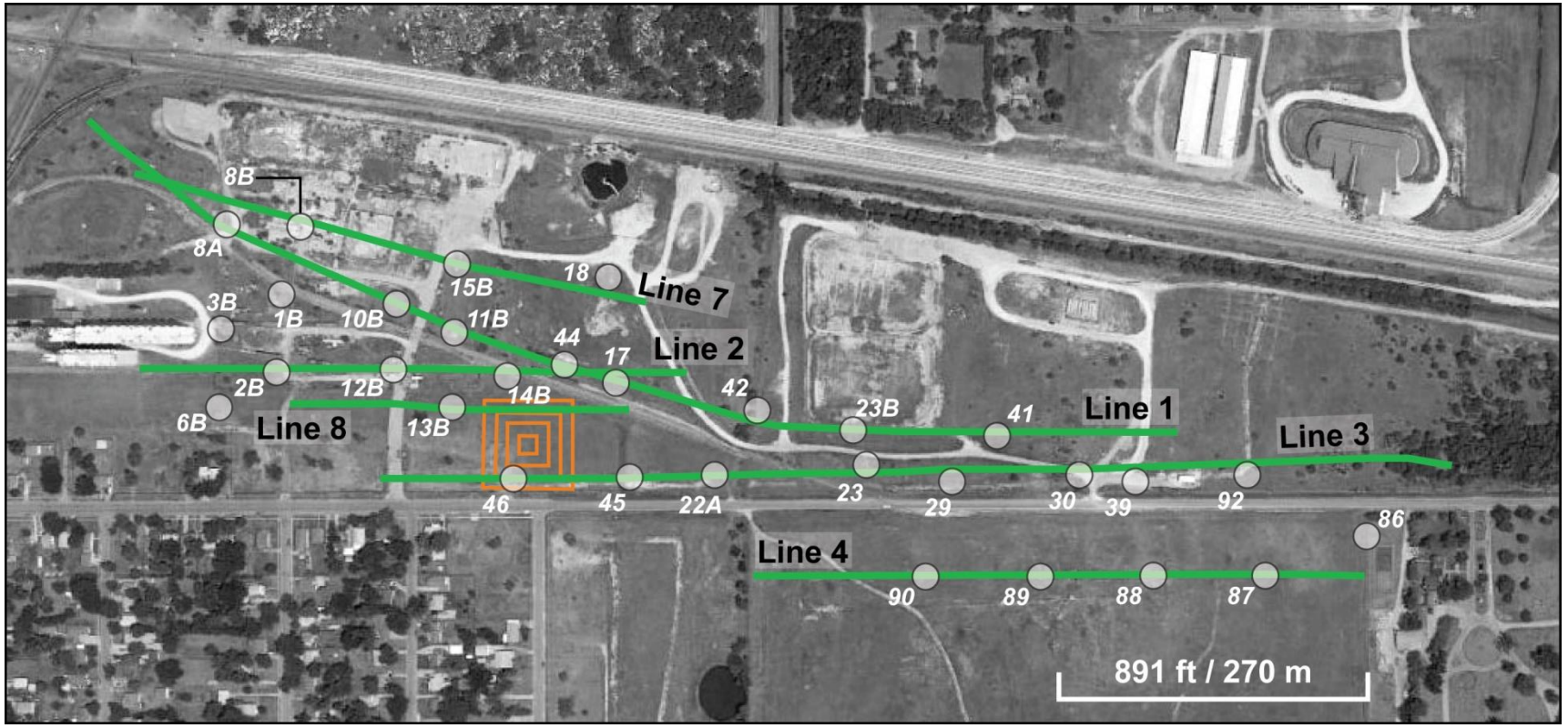

Figure 3. Aerial photo with GPS locations of seismic lines wells in the study area.

Table 1. Number of receivers, total lengths, and wells located on and near each seismic line acquired in this study.

	total # of receivers	total line length (m)	well(s) located directly on survey line	off-line well(s) in proximity of line
line 1	330	987	8A, 10B, 11B, 44, 17, 42, 23B, 41	1B, 8B
line 2	134	399	2B, 12B, 14B, 44, 17	3B, 6B
line 3	305	912	46, 45, 22A, 23, 29, 30, 39, 92	86
line 4	183	542	90, 89, 88, 87	86
line 7	150	447	8B, 15B	18
line 8	100	297	13B	n/a

Processing and Analysis

Data were processed using algorithms developed at the Kansas Geological Survey (KGS). The passive method used for this study is well published and provides good quality results at a similar nearby site (Park et al., 2004; Ivanov et al., 2013). Continuous acquisition records energy from energy sources at various orientations with respect to the seismic line. The 2-D grid was deployed to evaluate and optimize source alignment with respect to each 1-D seismic line to effectively identify void roofs with elevated stress and an elevated risk of vertical migration.

For each line, the surface wave amplitudes recorded by the 2-D grid were plotted as phase velocity versus frequency for a range of azimuths from 0 to 360 degrees with respect to the seismic line to determine which record had the best broad band, low frequency source with an azimuth near parallel to the line (Figure 4). The seismogram with optimum source characteristics was selected and divided into the shortest groups of receivers ("spread length") which provided dispersion patterns on phase velocity versus frequency plots with high amplitude fundamental mode Rayleigh wave energy and minimal higher-order surface wave interference

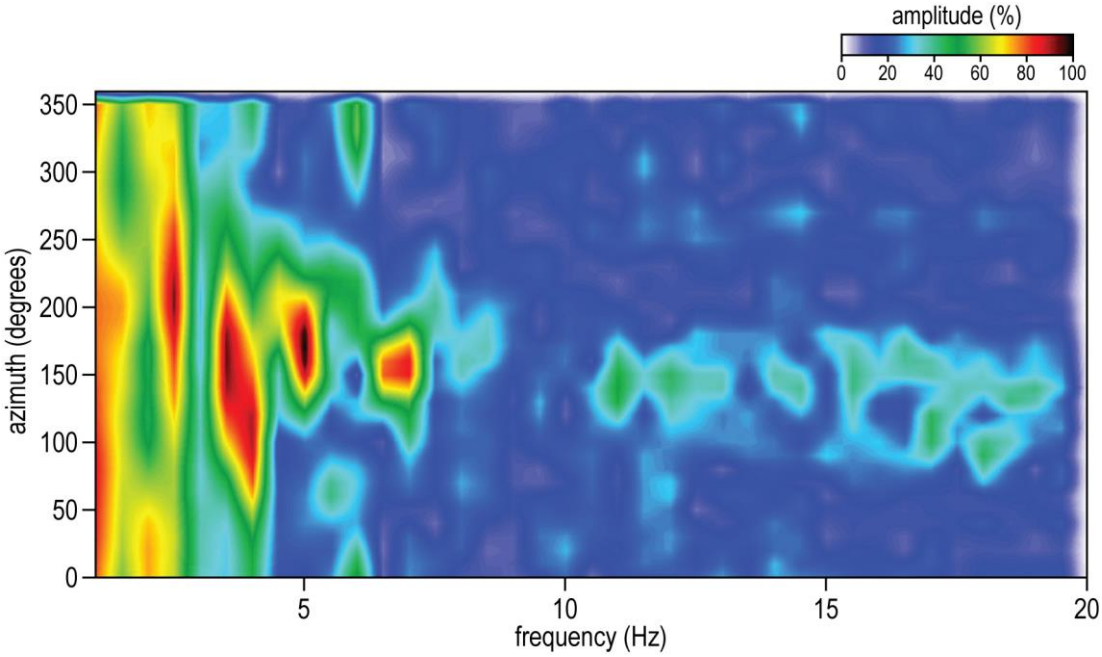

Figure 4. Azimuth plot indicating the direction of the dominant passive source energy (in degrees counter-clockwise from east). Here, the dominant passive source energy is centered on approximately 170°.

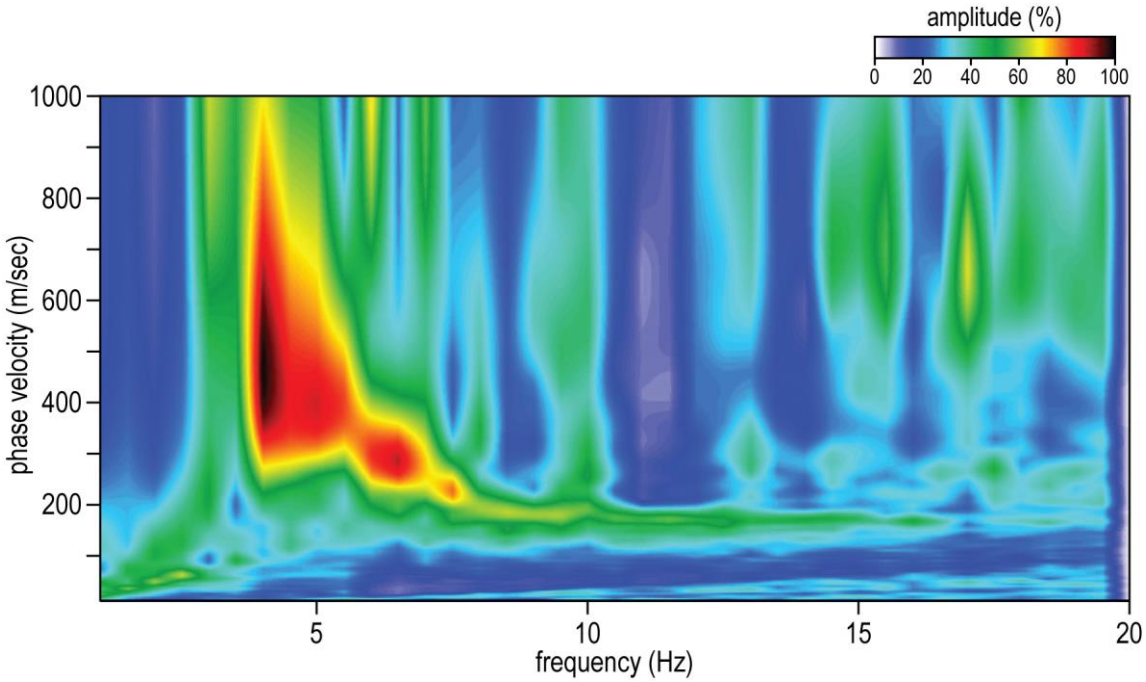

Figure 5. Representative dispersion pattern with high signal-to-noise ratio of the fundamental mode Rayleigh wave.

(Figure 5). Fundamental mode dispersion curves were picked and inverted to obtain a 2-D section of shear-wave velocity as a function of depth. The apparent velocity (v_{app}) is:

$$v_{app} = \frac{v_{act}}{(\cos\theta)} \quad (1)$$

where v_{act} is the actual seismic velocity and θ is the azimuth of the source with respect to the seismic line determined from the azimuth versus frequency plot. Thus, the increase in velocity (Δv) is:

$$\Delta v = \frac{1}{\cos\theta} - 1 \quad (2)$$

Equation 2 was used to calculate the increase in velocity due to the source azimuth for each line (Table 2).

Results and Observations

Line 1 is oriented NW-SE and is located directly over wells 8A, 10B, 11B, 44, 17, 42, 23B, and 41, and is in proximity to wells 1B and 8B (each are located approximately 30 m from the line between wells 8A and 10B). The velocity of the upper layer is approximately 150 meters per second (m/s) (Figure 6), which is consistent with the average Vs of unconsolidated sediment. At approximately 15 m, the Vs increases to 350 m/s, indicating the top of shale bedrock. The average depth of investigation on line 1 is 55 m, which is attributed to low

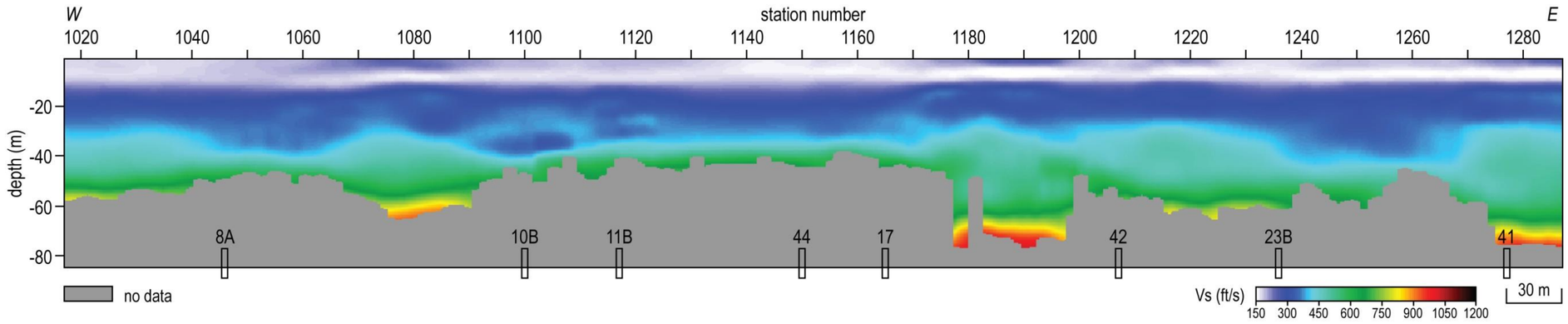

Figure 6. Shear-wave velocity profile from line 1. Approximate well locations are indicated at the bottom of the profile.

Table 2. Directions of the passive seismic sources and the seismic lines (in degrees counterclockwise from east), the relative angle of the source with respect to the line (θ), and the percent increase in apparent velocity (Δv) attributable to oblique source orientations.

	source orientation	line orientation	θ	Δv
line 1	163°	160°	3°	< 1%
line 2	180°	175°	5°	< 1%
line 3	180°	170°	10°	1.5%
line 4	180°	350°	10°	1.5%
line 7	166°	175°	9°	1.2%
line 8	180°	175°	5°	< 1%

fundamental mode Rayleigh wave signal at frequencies less than 4 hertz (Hz). Apparent variability in Vs within bedrock between 30-40 m is likely related variability in the signal-to-noise ratio of the fundamental mode and may not indicate changes in material properties. Velocities observed on the line 1 2-D Vs profile generally suggest a normal stress regime. An increase in Vs at 55 m depth is observed between stations 1072-1090, which may represent an off-line anomaly. The depth of investigation increases to nearly 80 m between wells 17 and 42 at stations 1176-1198, and near well 41 at stations 1274-1287, which may indicate elevated Vs within the dolomite at or near these locations.

Line 2 is oriented W-E and extends over wells 2B, 12B, 14B, 44, and 17, and is in proximity to wells 3B and 6B (each are located approximately 60 m from the west end of the line). The velocity of the uppermost layer is approximately 150 m/s (Figure 7), which is consistent with the average Vs of unconsolidated sediment. At approximately 15 m, Vs increases to 300 m/s, indicating the top of shale bedrock. Velocities at well 2B are consistent with the velocities obtained on line 56 in the August 2012 study. The depth of investigation increases from ~55 m on the west end of the line to 75-80 m centered on well 14B. In addition, Vs of the shale bedrock from 30-50 m is elevated approximately 10% between stations 2074-2046 relative to the rest of the line.

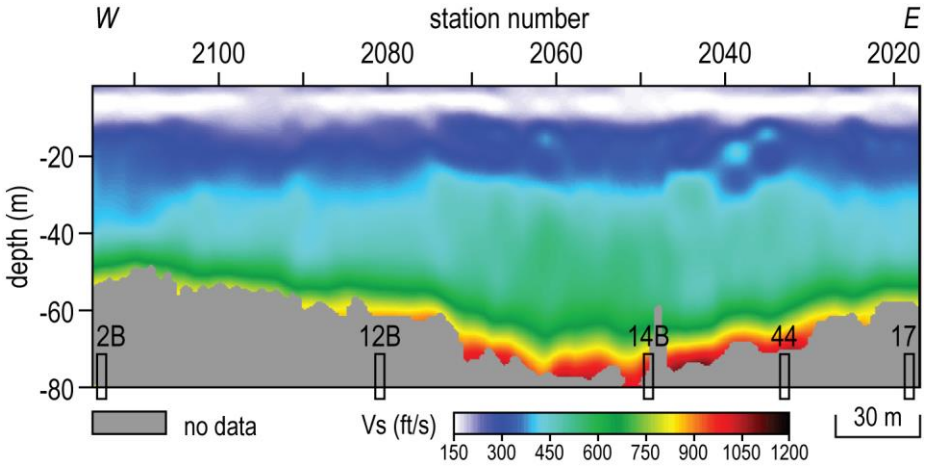

Figure 7. Shear-wave velocity profile from line 2. Approximate well locations are indicated at the bottom of the profile.

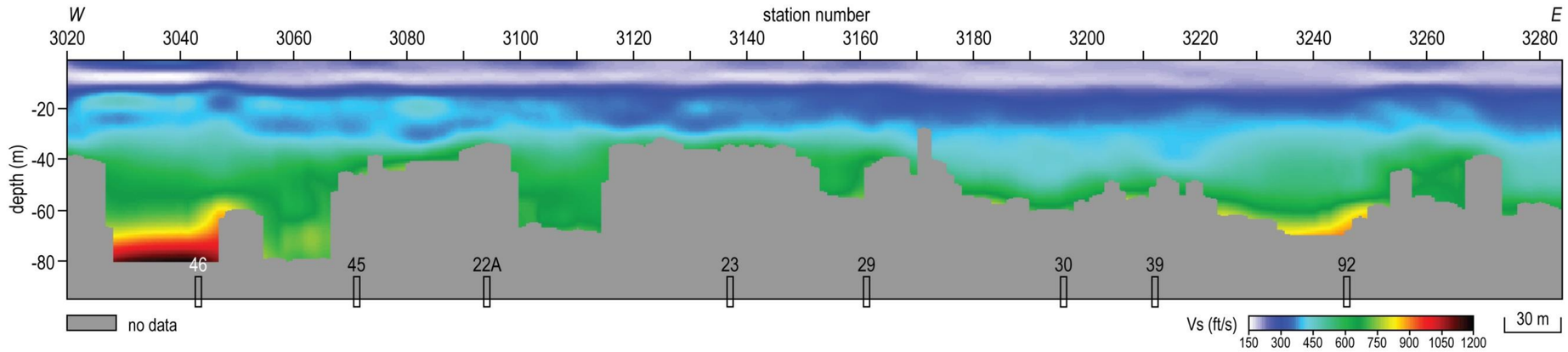

Figure 8. Shear-wave velocity profile from line 3. Approximate well locations are indicated at the bottom of the profile.

Line 3 is oriented W-E and extends over wells 46, 45, 22A, 23, 29, 30, 39, and 92, and is in proximity to well 86 (~60 m from the east end of the line). The velocity of the uppermost layer is approximately 150 m/s (Figure 8), which is consistent with the average Vs of unconsolidated sediment. At approximately 15 m, Vs increases to 350 m/s, indicating the top of shale bedrock. Similar to line 1, the average depth of investigation on line 3 is 55 m, which is attributed to low fundamental mode Rayleigh wave signal at frequencies less than 4 Hz. The majority of the 2-D Vs profile represents a normal stress regime with natural geologic variation. A slightly elevated velocity is observed near well 92 from stations 3224-3250 at a depth of 60 m. Near well 46 between stations 3028-3046, the shear velocity is elevated at 55-80 m, and the depth of investigation is almost 30 m deeper than average for this line.

Line 4 is oriented W-E and extends over wells 90, 89, 88, and 87, and is in proximity to well 86 (~45 m from the east end of the line). The velocity of the uppermost layer is approximately 150 m/s (Figure 9), which is consistent with the average Vs of unconsolidated sediment. At approximately 15 m, Vs increases to 300 m/s, indicating the top of shale bedrock. The 2-D Vs profile, in general, represents a normal stress regime with natural geologic variation.

Line 7 is oriented NW-SE and extends over wells 8B and 15B, and is in proximity to well 18 (24 m from the east end of the line). The velocity of the uppermost layer is approximately 150 m/s (Figure 10), which is consistent with the average Vs of unconsolidated sediment. At approximately 15 m, Vs increases to 325 m/s, indicating the top of shale bedrock. The average depth of investigation on this line is approximately 75 m. Elevated shear-wave velocity is observed centered on well 15B and, to a lesser degree, 8B. The velocity inversions at a depth of 10-25 m at stations 7094-7106 and 7048-7068 are most likely artifacts of the inversion process and, therefore, low confidence.

Line 8 is oriented W-E and is centered on well 13B. The velocity of the uppermost layer is approximately 150 m/s (Figure 11), which is consistent with the average Vs of unconsolidated sediment. At approximately 15 m, Vs increases to 325 m/s, indicating the top of shale bedrock. The 2-D Vs profile represents a normal stress regime with natural geologic variation. Reduced depth of investigation on the west end of the line is attributed to the reduced signal-to-noise ratio of the fundamental mode dispersion pattern below 4 Hz.

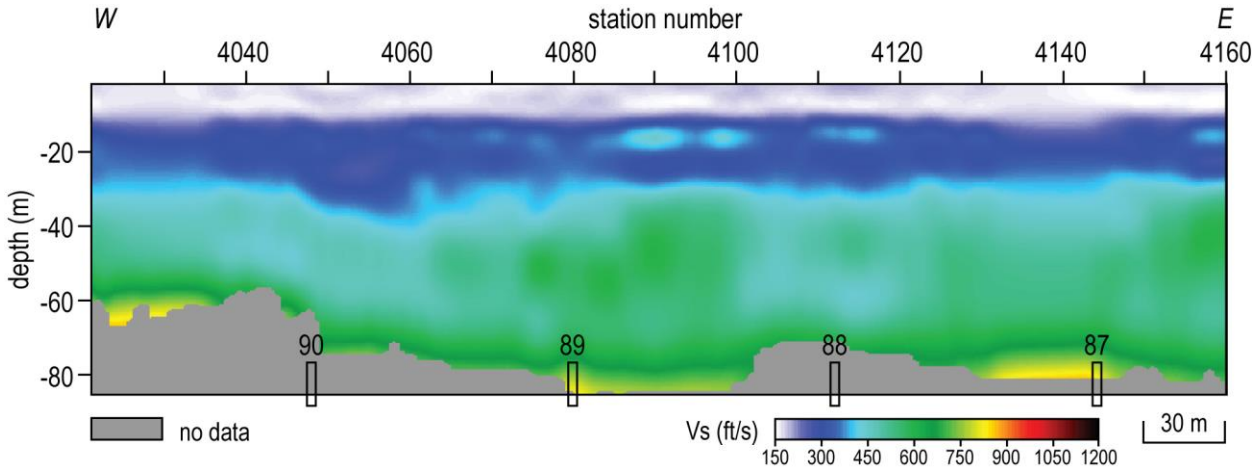

Figure 9. Shear-wave velocity profile from line 4. Approximate well locations are indicated at the bottom of the profile.

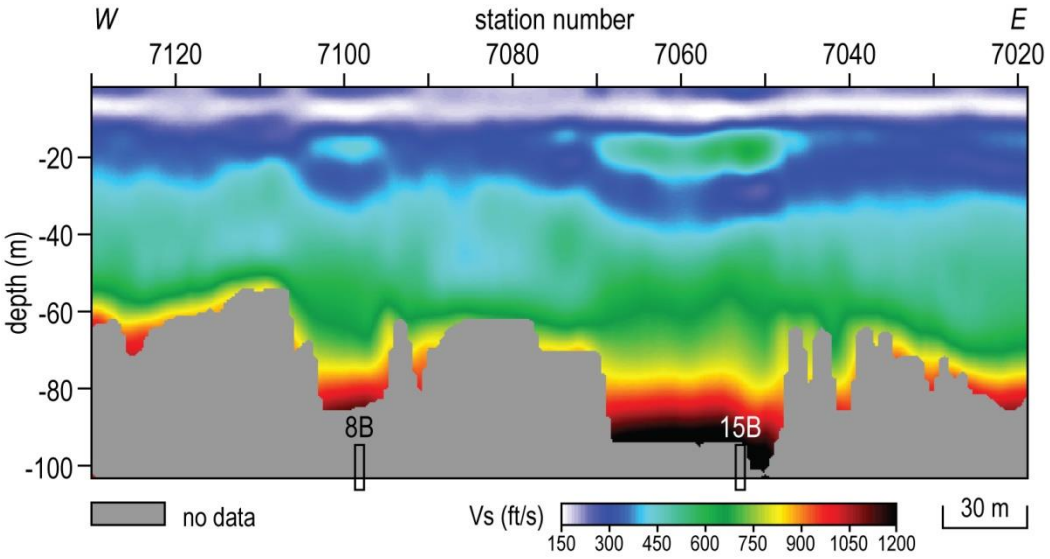

Figure 10. Shear-wave velocity profile from line 7. Approximate well locations are indicated at the bottom of the profile.

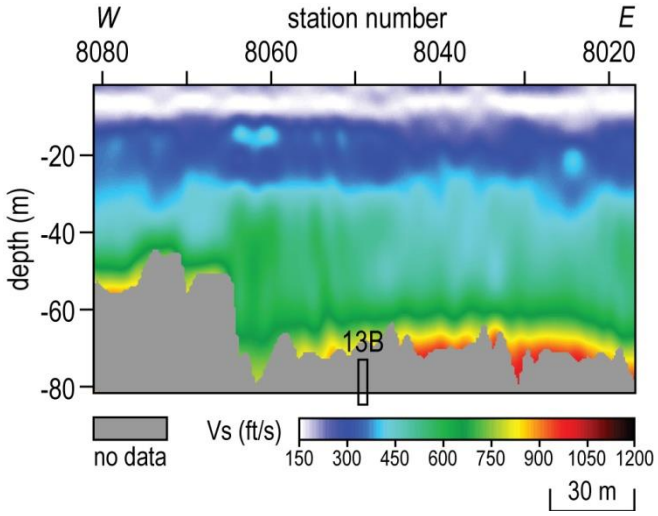

Figure 11. Shear-wave velocity profile from line 8. Approximate well locations are indicated at the bottom of the profile.

Comprehensive Interpretation

Wells 2B, 8A, 10B, 11B, 12B, 13B, 17, 22A, 23, 23B, 29, 30, 39, 42, 44, 45, 87, 88, 89, 90

Velocity profiles acquired directly over these wells likely represent natural geologic variation and a normal stress regime.

Wells 3B, 6B, 86, 18

Acquired seismic lines or processing spread lengths used in the present study do not extend directly over these wells. However, significant changes in Vs would likely affect surface

wave propagation and apparent velocity on lines 1, 2, and 7. The 2-D Vs profiles of these lines do not appear to indicate significant off-line anomalies associated with these wells.

Wells 14B, 41, and between wells 17 and 42

Increased depths of investigation indicate that longer surface wave wavelengths were recorded at well 14B on line 2 (Figure 7), well 41, and between wells 17 and 42 on line 1 (Figure 6). Wavelength is a function of Rayleigh wave phase velocity:

$$\lambda = \frac{v}{f}. \tag{3}$$

An increase in wavelength may suggest an increase in velocity at depth. Changes in dispersion patterns between wells at these locations support this observation. The velocity observed at 70-80 m is consistent with the depth and velocity expected for the three finger dolomite and likely represents natural geologic variation. However, increased penetration depth suggests there is something unique to these areas—possibly depositional variability or localized variability related to void characteristics—relative to the remainder of lines 1 and 2. Lack of a corresponding velocity increase within the overburden indicates that the voids associated with these wells have not propagated beyond the dolomite. These anomalous zones are not necessarily cause for concern, but may warrant future monitoring to increase confidence in the interpretation.

Well 92

The shear-wave velocity near well 92 on line 3 is slightly elevated at a depth of 60 m (Figure 8). Although confidence in Vs on this line is somewhat lower due to lower signal-to-noise ratio of the fundamental mode Rayleigh wave, dispersion patterns suggest an increase in velocity consistent with the 2-D Vs profile. Because this anomaly may represent elevated Vs within the shale bedrock, it may warrant inclusion in future investigations to characterize any dynamic Vs changes and increase confidence in the interpretation.

Wells 1B and 8B

An increase in Vs at approximately 55 m depth is observed on line 1 between stations 1072-1090 (Figure 6). This general location is in proximity to off-line wells 1B (25 m south of station 1068) and 8B (25 m northeast of station 1067). On line 7, elevated Vs are observed at well 8B (Figure 10). Although elevated Vs at well 1B cannot be ruled out with complete certainty, the off-line anomaly observed on line 1 is likely related to well 8B.

The anomaly at well 8B on line 7 is relatively localized (spanning a total distance of approximately 50 m) and indicates a slightly elevated velocity (~10%) at a depth of 60 m. The velocity trend suggests no failure or reduction of strength at the surface of the bedrock. Based on the size, geometry, and relative velocity, this anomaly does not suggest vertical migration.

Wells 15B and 46

The shear-wave velocity near well 15B on line 7 (Figure 10) and well 46 on line 3 (Figure 8) is elevated at a depth of 55-80 m or greater. The relative velocity is approximately 25-30% greater than velocities observed within this depth range on other lines (e.g. east end of lines 1 and 8). These anomalous velocity zones extend a total horizontal distance of 60 m for well 15B and 70 m for well 46. A low-velocity anomaly is not observed at the depths imaged,

indicating that these voids have not vertically migrated beyond the three finger dolomite. Elevated velocity likely represents increased stress over an under-supported roof at these locations. The velocity trend suggests no failure or reduction of strength at the surface of the bedrock and the possibility of failure does not appear to be imminent. We recommend these wells be included in future investigations at this site to monitor for possible changes in Vs associated with void dynamics.

Conclusions

The shear-wave velocity directly over or in proximity to the majority of the wells in this study represents natural geologic variation and a normal stress regime. Increased depths of investigation and maximum surface wave wavelengths were observed near wells 14B and 41, and between wells 17 and 42. Shear-wave velocities at these locations are consistent with the velocity trend expected for bedrock at this site and likely represent natural variability. However, increased wavelength may be associated with elevated Vs at depth and/or an off-line anomaly. Future monitoring at these locations would enhance the dataset and improve confidence in the interpretation.

Elevated shear-wave velocity is observed at wells 8B, 15B, 46, and possibly well 92 at depths of 55 m and greater, implying elevated stress and voids with under-supported roof spans at these locations. Although the stress is anomalous, it does not appear to be dramatic enough to imply migration or imminent collapse; voids can be totally benign and possess the observed shear-wave velocity characteristics. We recommend including these wells in future investigations to monitor for and evaluate changes in Vs associated with void dynamics.

References

Dellwig, L.F., 1963, Environment and mechanics of deposition of the Permian Hutchinson Salt Member of the Wellington shale: Symposium on Salt, Northern Ohio Geological Society, p. 74-85.

Holdoway, K.A., 1978, Deposition of evaporites and red beds of the Nippewalla Group, Permian, western Kansas: Kansas Geological Survey Bulletin 215.

Ivanov, J., R.D. Miller, S.L. Peterie, J.T. Schwenk, J.J. Nolan, B. Bennett, B. Wedel, J. Anderson, J. Chandler, and S. Green, 2013, Enhanced Passive Seismic Characterization of High Priority Salt Jugs in Hutchinson, Kansas: preliminary report to Burns & McDonnell Engineering Company.

Kulstad, R.O., 1959, Thickness and salt percentage of the Hutchinson salt; in, Symposium on Geophysics in Kansas: Kansas Geological Survey Bulletin 137, p. 241-247.

McGuire, D., and B. Miller, 1989, The utility of single-point seismic data: In Geophysics in Kansas, D.W. Steeples, ed.: Kansas Geological Survey Bulletin 226, p. 1-8.

Merriam, D.F., 1963, The Geologic History of Kansas: Kansas Geological Survey Bulletin 162, 317 p.

Merriam, D.F., and C.J. Mann, 1957, Sinkholes and related geologic features in Kansas: Transactions of the Kansas Academy of Science, v. 60, p. 207-243.

Park, C., R. Miller, D. Laflen, N. Cabrillo, J. Ivanov, B. Bennett, and R. Huggins, 2004, Imaging dispersion curves of passive surface waves [Exp. Abs.]: Annual Meeting of the Soc. of Expl. Geophys., Denver, Colorado, October 10-15, p. 1357-1360.

Swineford, A., 1955, Petrography of upper Permian rocks in south-central Kansas: State Geological Survey of Kansas Bulletin 111, 179 p.

Walters, R.F., 1978, Land subsidence in central Kansas related to salt dissolution: Kansas Geological Survey Bulletin 214, 82 p.

Whittemore, D.O., 1990, Geochemical identification of saltwater contamination at the Siefkes subsidence site: Report for the Kansas Corporation Commission.

Whittemore, D.O., 1989, Geochemical characterization of saltwater contamination in the Macksville sink and adjacent aquifer: Kansas Geological Survey Open-file Report 89-35.